HEAVILY ALTERED ALUMINUM-RICH LIGHT-TONED FLOAT ROCKS IN JEZERO CRATER.

C. Royer[1], C. C. Bedford[2], R. C. Wiens[2], J. R. Johnson[3], B. H. N. Horgan[2], A. Broz[2], O. Forni[4], S. Connell[2], L. Mandon[5], B. S. Kathir[6], E. M. Hausrath[7], A. Udry[7], J. M. Madariaga[8], E. Dehouck[9], R. B. Anderson[10], P. Beck[5], O. Beyssac[11], É. Clavé[12], S. M. Clegg[13], E. Cloutis[14], T. Fouchet[15], T. S. J. Gabriel[10], B. J. Garczynski[16], A. Kildaras[2], H. T. Manelski[2], L. Mayhew[17], J. Nuñez[3], A. M. Ollila[13], S. Schröder[12], J. I. Simon[18], U. Wolf[13], K. M. Stack[16], A. Cousin[4], and S. Maurice[4]. [1]LATMOS, CNRS, France (*clement.royer@latmos.ipsl.fr*); [2]Purdue Univ., USA, [3]JHU-APL, USA, [4]IRAP, CNRS, France, [5] IPAG, CNRS, France, [6]Western Washington Univ., USA, [7]Univ. of Nevada, Las Vegas, USA, [8]Univ. of the Basque Country, Spain, [9]LGL-TPE, Univ. de Lyon, France, [10]United States Geological Survey, USA, [11]IMPMC, CNRS, France, [12]DLR, Germany, [13]LANL, USA, [14]Univ. of Winnipeg, Canada, [15]LESIA, CNRS, France, [16]JPL, Caltech, USA, [17]Univ. of Colorado, USA, [18]NASA Johnson Space Center, USA.

Introduction: Since landing in Jezero crater, the Mars 2020 Perseverance rover has encountered light-toned float rocks (LTF) dispersed across the crater floor, Jezero delta, and the crater rim (see Fig. 1). SuperCam [1,2] observations show elemental compositions unlike anything else found on Mars, consisting almost entirely of Al and Si oxides. In Mastcam-Z [3] images, over 4,000 candidate LTFs have been identified, primarily ranging from gravel to pebble size, occasionally appearing as fine sand, coarse sand, and boulders (up to 40 cm). This study utilizes imaging, chemical, and mineralogical data obtained from SuperCam and Mastcam-Z aboard Perseverance to elucidate the origins of these float rocks.

Methods: SuperCam has analyzed 19 LTFs targets in total: 18 have been analyzed using RMI, LIBS and VISIR, 2 targets have been analyzed with Raman, and 1 target is RMI-only. VISIR spectra were modeled to determine the best mineral assemblages describing the data. The modeling method we employed relies on the use of linear combinations of reflectance spectra derived from a library of laboratory spectra. The method involves combining a large number of spectral endmembers to account for the variability of reflectance of each species based on its state (powders of various grain sizes, slabs), observation conditions, and purity.

Results: Most of the LTFs show very high Al_2O_3 abundances (~ 25 to 45 wt%) relative to other rocks in Jezero crater and Mars (Fig. 2). Only one float has high SiO_2 abundances and little Al_2O_3 (AEGIS_0910A) but is situated at the end of the negative Al_2O_3-SiO_2 regression line, potentially representing the high-SiO_2 endmember. All LTFs have very low abundances of cations FeO_T, MgO, CaO, Na_2O (< 5 wt%) and some of them exhibit a singular Ni enrichment despite the relative absence of Fe [4].

Based on LIBS results and initial VISIR absorption bands analysis, the spectral modeling library contains only species exhibiting absorption bands compatible with observations (1.4, 1.9, 2.2, 2.39 µm) and having very low Fe and Mg, and high Al contents: kaolinite, halloysite, Al-phyllosilicates (montmorillonite, illite), Al-hydroxide, hydrated silica (opal-A), spinel, Al-silicate (cordierite, sillimanite), and zeolite. Even though sulfur is not detected a priori by LIBS, given its detection threshold close to 10 % [5], sulfates were included in the library to account for an observed broadening of the 1.9 µm band relative to other candidate minerals. VISIR modeling results have been used as basis for subsequent stoichiometric modeling of LIBS data (see [6]).

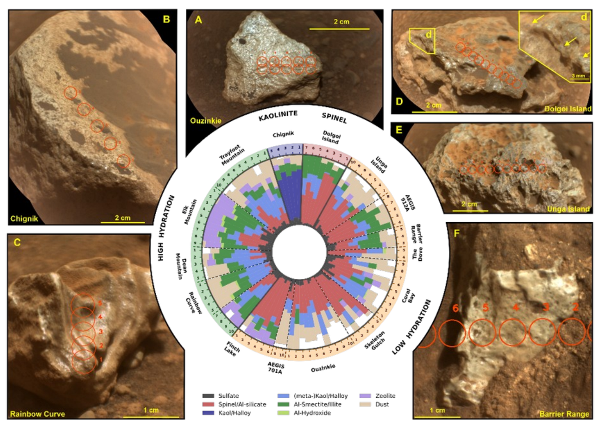

Figure 1: Plot of IR mixing coefficients for each target alongside RMI images highlighting the textural classes in the LTFs.

The VISIR spectra suggest the presence of multiple aqueous alteration phases, notably displaying the band at 2.19-20 µm attributed to Al-OH and with varying intensities of bands at 1.4 and 1.9 µm associated with H_2O and OH. The VISIR observations are classified into four spectral classes:

- The "kaolinite bearing" class includes only the Chignik target exhibiting absorption doublets at 1.4 and 2.2 µm diagnostic of kaolinite and/or halloysite presence. The low contrast of these bands compared to pure kaolinite suggests lower mineral crystallinity or the presence of other Al-rich phases.
- The "hydrated" class corresponds to rocks with spectra showing marked absorption bands at 1.4, 1.9, and 2.2 µm, indicative of water and hydroxyl

presence but without doublets. Their texture is often spotted with a dark material or layered (e.g., Fig. 1B and C)

- Conversely, the "low hydration" class is representative of rocks with featureless VISIR spectra or very weak absorption bands. This class corresponds to the highest Al_2O_3 contents in the dataset. The overall spectral shape (slightly concave) is also consistent with the presence of spinel and/or aluminosilicates. Their texture varies from a smooth white-toned to a rougher surface (e.g., Fig. 1A, E and F)
- The "spinel-bearing" class includes only the Dolgoi Island target, whose spectrum exhibits the broad absorption band at 2 µm characteristic of spinel.

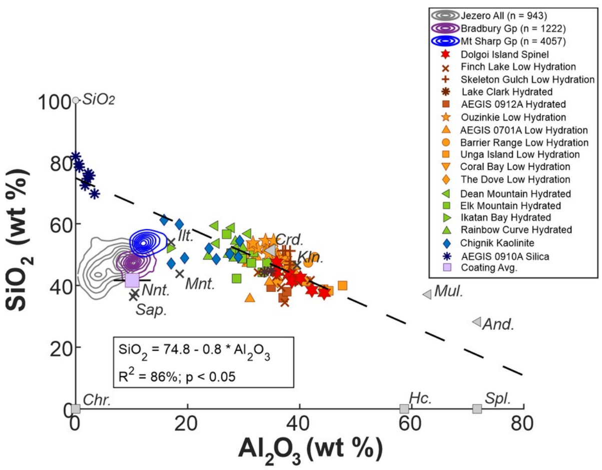

Figure 2: *SiO_2 versus Al_2O_3 for the LTFs. Hydrated floats are in blue/green, floats with the least hydration are in yellow/red. Different shapes relate to different rocks. Also plotted are density contours showing the Jezero crater bedrock and ChemCam data for Gale crater geological units for comparison.*

Discussion: The LTFs exhibit a chemical and mineralogical composition that reflects extensive aqueous alteration and leaching followed by dehydration indicative of high-temperature metamorphism. The high concentrations of Al_2O_3 along with depleted FeO_T, MgO, CaO, and Na_2O, coupled with the presence of abundant kaolinite and Al-clays, suggest significant leaching akin to processes observed in tropical weathering soil profiles or linked to hydrothermal activity [e.g., 7]. In the Nili Fossae region near the Jezero crater watershed, several exposed sections of Noachian crust display tropical weathering profiles (characterized by kaolinite at the surface transitioning to Fe/Mg phyllosilicates) [8]. It is probable, therefore, that the mineralogy of the hydrated classes and the enrichment in Al_2O_3 originate from a similar Noachian crustal source. Comparative studies using terrestrial analogue paleosols are ongoing to constrain this hypothesis [9].

Certain LTFs exhibiting signs of dehydration, increased Al_2O_3 enrichment, and mineral assemblages containing metakaolinite, aluminosilicate, and spinel indicate extensive leaching due to aqueous alteration processes followed by heating. Studies of high-temperature contact metamorphism on Earth demonstrate that at temperatures around ~1000°C, rocks rich in Al_2O_3 and SiO_2 can form assemblages featuring cordierite, mullite/metakaolinite, and spinel [10,11].

Two potential heat sources are likely responsible for metamorphosing these rocks: contact metamorphism from a large igneous intrusion or impact metamorphism. The Jezero crater watershed contains several large impact craters associated with kaolinite weathering horizons [8]. Additionally, prominent linear features with fractured, light-toned margins in northeast Syrtis Major may be linked to contact metamorphism caused by igneous intrusions [12]. Consequently, both scenarios are plausible and may be associated with hydrothermal activity capable of producing silica-rich rocks like AEGIS_0910A. The scattered distribution of these rocks within Jezero suggests they were transported late in the geological history of the crater, either as impact ejecta or by late-stage flood or fluvial processes.

References: [1] Maurice, S. et al. (2021) *Space Sci. Rev.*, *217*, 47. [2] Wiens, R.C. et al. (2021) *Space Sci. Rev.*, *217*, 47. [3] Bell III, J. F. et al. (2021) *Space Sci. Rev*. 217, 24 [4] Forni, O. et al. *this meeting*. [5] Anderson, R.B. et al., (2022) *Spectrochimica Acta Part B: Atomic Spectroscopy*, 188, p. 106347. [6] Madariaga, J. M. et al. *this meeting*. [7] Gaudin, A. et al. (2011) *Icarus*, 216, 1. [8] Carter J. et al. (2015) Icarus, 248, 1. [9] Broz, A. et al. *this meeting*. [10] Grapes, R. (2010) *Springer Science & Business Media*. [11] Del Moro, S. et al. (2011) *Journal of Petrology*, 32, 3. [12] Bramble, M. S. et al. (2017) *Icarus*, 291, 1.